REGULATION OF MELANOGENESIS BY THE AMINO-ACID TRANSPORTER SLC7A5.

Céline Gaudel[1,2], Frederic Soysouvanh[2], Justine Leclerc[2], Karine Bille[2], Chrystel Husser[2], François Montcriol[1], Corine Bertolotto[2]* and Robert Ballotti[2]*

1 Nunii Laboratoire, Grasse Biotech, Grasse, France

2 Université Nice Côte d'Azur, C3M, INSERM, U1065, Biology and pathologies of melanocytes, Nice, France

Corresponding should be addressed to : INSERM U1065, Team1, 151 rt de Saint Antoine de Ginestière, Hopital Archet 2, 06200, Nice. Email: ballotti@unice.fr

* Equal contribution

SHORT TITLE. SLC7A5 regulates melanogenesis.

ABBREVIATIONS: TYR: tyrosinase; TYRP1: tyrosine-related protein 1; DCT: dopachrome tautomerase; L-DOPA: L-3,4-dihydroxyphenylalanine.

ABSTRACT

Integration of ChIPseq and microarray data allowed to identify new MITF target genes, among which, the amino acid transporter, SLC7A5. We showed that siRNA-mediated SLC7A5 knock-down decreased pigmentation in B16F10 cells, without affecting morphology nor dendricity. Treatment with the SLC7A5 inhibitors BCH, or JPH203, also decreased melanin synthesis in B16F10 cells. Our findings indicated that BCH was as potent as reference depigmenting agent, Kojic Acid, but acted through a different pathway not affecting tyrosinase activity. BCH also decreased pigmentation in human MNT1 melanoma cells or normal human melanocytes. Finally, we tested BCH on a more physiological model, using reconstructed human epidermis and confirmed a strong inhibition of pigmentation demonstrating the clinical potential of SLC7A5 inhibition and positioning BCH as a depigmenting agent suitable for cosmetic or dermatologic intervention in hyperpigmentation diseases.

INTRODUCTION

The melanin pigments, which are responsible for the color of the skin in humans, are synthesized by melanocytes in the epidermis. Therefore, the molecular mechanisms that control the growth and differentiation of melanocytes have an influence on skin pigmentation.

Melanin synthesis, or melanogenesis, is tightly regulated by tyrosinase (*TYR*), a melanocyte-specific enzyme, that catalyzes many reactions, including the rate-limiting step of melanogenesis, the hydroxylation of tyrosine to L-3,4-dihydroxyphenylalanine (L-DOPA). Other enzymes are involved in melanogenesis. For example, tyrosinase-related protein-1 (*TYRP1*) has a DHICA oxidase activity and the enzyme coded by *DCT* has a Dopachrome Tautomerase activity. TYRP1 and DCT are involved in the synthesis of eumelanin, the black-brown melanin responsible for photo-protection against noxious effect of UV radiations (Miyamura *et al.*, 2007).

Melanogenesis occurs in specialized organelles called melanosomes. They are related to lysosomes but contain several specific proteins that allow biogenesis and specification of these vesicles, such as PMEL17, MART1, GPR143, SLC45A2, SLC24A5 and many others (Kondo and Hearing, 2011). The melanocytes are equipped with a specific transport machinery of intracellular vesicles, involving RAB27A, MLPH and MYOVa that allows melanosomes to accumulate at the ends of melanocyte dendrites. This process favors melanosome transfer to neighboring keratinocytes and uniform skin pigmentation (Hume and Seabra, 2011; Sitaram and Marks, 2012).

To date, more than 250 genes have been involved directly or indirectly in the control of skin pigmentation, in humans (Baxter *et al.*, 2019). Among these genes, MITF plays a key role in these developmental processes, because it is at the crossroads of all the signaling pathways involved in the development of melanocytes. MITF is a transcription factor that regulates the

expression of many genes involved in the proliferation, survival and migration of melanocytes, such as CDK2, BCL2 and MET (non-exhaustive list). Other MITF target genes are directly involved in melanocyte differentiation processes. MITF controls the expression of all the genes encoding the proteins evoked above that are required for melanin synthesis, melanosome biogenesis, and melanosome transport. MITF ensures the coordinated regulation of all these processes that are necessary for optimal differentiation and physiological skin pigmentation (Cheli *et al.*, 2010; Goding and Arnheiter, 2019).

In this study, we aimed at identifying new genes involved in pigmentation, that might be new molecular targets for depigmenting agents to be used in the treatment of hyper-pigmentation diseases, such as melasma or actinic lentigo. As a large portion of MITF target genes identified so far does not have known functions, their involvement in melanocyte differentiation and pigment synthesis deserves to be evaluated.

Combined bioinformatics analysis of public ChIP-Seq and transcriptomic data allowed us to identify new direct MITF target genes. Further analysis, pointed-out to SLC7A5 as a new MITF target and pigmentation gene. SLC7A5 encodes an amino-acid transporter that genetic or pharmacologic inhibition decreases melanin pigment synthesis and allows depigmentation of reconstructed pigmented epidermis, pointing-out to SLC7A5 as a new target in the treatment of hyper-pigmentation pathologies.

RESULTS

Identification of new direct MITF target genes

First, to identify genes bound by MITF and expression of which covaries with MITF, we combined analysis of the MITF ChIP seq experiment (Laurette *et al.*, 2015) with that of the

CCLE melanoma panel (Broad Institute). This analysis identified 1068 pics in 946 genes. Gene ontology analysis of these genes showed an enrichment of terms associated with melanin synthesis (Supplementary Table 1), strengthening the role of MITF in positive regulation of pigmentation genes.

Among the 946 genes, we searched for those that are down-regulated by MITF siRNA in both 501Mel human melanoma cells and B16F10 mouse melanoma cells. We found 5 genes (Supplementary Table 2) that fulfil all these criterions. Among these genes, TYR, RAB27A and MLPH were already described as involved in pigmentation. Two additional genes were identified, ST3GAL6 and SLC7A5 whose functions in pigmentation were not documented so far.

First round of functional analysis using siRNA to *St3gal6* and *Slc7a5* showed that *St3gal6* silencing inhibited proliferation of B16F10 melanoma cells (not shown), while the inhibition of *Slc7a5* expression had no significant effect on cell proliferation (Supplementary Figure 1a and b). Therefore, *Slc7a5* was selected for further studies.

Validation of *SLC7A5* as a MITF target

A UCSC browser image capture of the SLC7A5 promoter region from MITF (Black) (Laurette *et al.*, 2015), H3K27ac and H3K4me3 (purple) (Ohanna *et al.*, 2018) ChIP-seq experiments (Figure 1a) confirmed that MITF bound to the SLC7A5 promoter, and overlap histone activating epigenetic marks. Then, transfection of B16F10 melanoma cells with MITF siRNA showed a decrease in Mitf and Slc7a5 expression, both at messenger (Figure 1b) and protein level (Figure 1c) demonstrating that Slc7a5 is a new Mitf target gene. MITF silencing also decreased *SLC7A5* expression in 501Mel cells (Supplementary Figure 2)

siRNA-mediated *Slc7a5* knock-down inhibits melanogenesis in B16F10 cells.

Then we studied the effects of *Slc7a5* silencing on pigmentation in B16F10 melanoma cells. Cells transfected with control (siCt) or *Slc7a5* (siSlc7a5) siRNA were incubated with cAMP-elevating agents (Forskolin, 20µM, IBMX 100µM) to increase melanogenesis. 48 hours later, western blot analysis confirmed the strong inhibition of Slc7a5 expression at protein level, by 2 different si*Slc7a5* (Figure 2a). On bright field images (Figure 2b), a clear inhibition of cells pigmentation was seen after *Slc7a5* silencing. This observation was confirmed by measurement of melanin content (Figure 2c). Both siRNA directed against *Slc7a5* resulted in a 60% decrease in melanin content. Unexpectedly, *Slc7a5* silencing led to a slight and barely significant increase in Tyrosinase (Tyr) and Dct, while the effect was much more pronounced for Tyrp1 expression. No significant effect was observed for Rab27a expression (Supplementary Figure 3a). qPCR analyses demonstrated that siSlc7A5 effectively inhibited Slc7a5 mRNA level, but did affect significantly the expression of Tyr, Tyrp1, Dct and Rab27a (Supplementary Figure 3b). Immunofluorescence studies of Tyrp1 expression showed that *Slc7a5* silencing did not affect drastically cells morphology or dendricity and confirmed the increased expression of Tyrp1 (Figure 2e). As Tyrp1 expression is clearly localised at the cell periphery, *Slc7a5* silencing does not seem to affect melanosome transport.

Pharmacological inhibiton of SLC7A5 decreases melanin content in B16F10 cells.

Next, we investigated the effects of pharmacological inhibitors of SLC7A5, BCH, and JPH203 that is now in clinical trial as an anti-cancer drug.

First, dose response experiments showed that BCH, up to 10mM did not affect significantly B16F10 cell viability (Figure 3a). Evaluation of melanin content showed a significant inhibition of melanin production in B16F10 cells, by BCH at 5mM (25%), and 10mM (60%) (Figure 3b). Bright field images confirmed that BCH inhibited pigmentation at 10mM (Figure 3c). Immunofluorescence with Tyrp1 antibody showed that BCH at 10mM did not obviously alter morphology of the cells (Figure 3d). As it was the case with the siRNA directed against *Slc7a5*,

we observed a consistent increase in Tyrp1 labelling. Western blot analysis confirmed a dose-dependent increase in Tyrp1 expression in response to BCH, while other melanogenesis proteins, such as Tyrosinase or Rab27a, were not affected consistently by BCH. BCH did not affect Slc7a5 expression (Supplementary Figure 4a).

Strengthening this observation, JPH203 at 10 and 50 µM, also efficiently inhibited pigmentation in B16F10 cells at doses that did not inhibit cell proliferation (Supplementary Figure 4b and c). Together these observations confirmed the involvement of *Slc7a5* in melanogenesis and the possible use of pharmacological inhibition of *Slc7a5* as depigmenting strategy.

Comparison of BCH and Kojic Acid effects on pigmentation

Next, we compared the effects of BCH to that of a well-known reference depigmenting agent, Kojic Acid. Dose response experiments confirmed the inhibition of melanogenesis by Kojic acid (Figure 4a), at doses that did not affect cell proliferation (Figure 4b). At 1mM, we observed an inhibition of 60% of melanin content. This effect is comparable to that observed in B16F10 cells in response to BCH. Furthermore, treatment of B16F10 cells with Kojic Acid (1mM), inhibited tyrosinase activity, while BCH (10mM) did not (Figure 4c). Then, when added directly in cell lysates during the DOPA oxidase assay (Figure 4d), Kojic Acid, but not BCH, inhibited tyrosinase activity. Therefore, we can conclude that BCH is as potent as Kojic Acid to inhibit melanogenesis in B16F10 melanoma cells, and that BCH does not inhibit tyrosinase activity.

BCH inhibited pigmentation in MNT1 human melanoma cells, normal human melanocytes, and reconstructed human pigmented epidermis.

Next, we verified the effects of BCH on human cells and on more physiological models such as normal melanocytes and reconstructed epidermis. First, using highly pigmented human

melanoma cells, MNT1 (Figure 5a) and pigmented normal human melanocytes (NHM) (Figure 5b), we confirmed that in both cell types, BCH significantly decreased melanin production. Then using reconstructed pigmented epidermis containing both melanocytes and keratinocytes, we clearly observed that BCH treatment inhibited pigmentation, as shown by macroscopic images (Figure 5c) and confirmed by bright field microscopic images (Figure 5d) of the epidermis. Additionally, Fontana Masson staining of epidermis sections demonstrated the absence of pigmented melanocytes in reconstructed epidermis exposed to BCH (Figure 5e). Finally, the quantification of melanin content confirmed a statistically significant decrease in melanin content in reconstructed epidermis treated with BCH (Figure 5f).

DISCUSSION

Pathologies associated with melanocytes dysfunction can lead to depigmentation as in vitiligo or hyper-pigmentation such as age spots (actinic lentigo) or melasma. These pigmentary defects do not endanger the lives of those affected but have a significant psychological impact. Until now, only heavy dermatological approaches have shown a real effectiveness in the treatment of pigmentary pathologies, vitiligo, melasma and actinic lentigo. The cosmetic approaches already used in the context of hyperpigmentation pathologies mainly target tyrosinase, a key enzyme in melanin synthesis, and/or the transfer of melanin to keratinocytes. These treatments show low efficiency.

In this study, using a very stringent bioinformatic analyses, we identified new MITF target genes ST3GAL6 and SLC7A5, function of which in pigmentation has never been studied. Of course, the list generated by our analyses does not contain all the known MITF target genes but can be easily increased by applying more tolerant filters.

SLC7A5 encodes for a member (LAT1) of the L-Type amino-acid transporter family that is specialized in the transport of histidine, tryptophan and tyrosine, in addition to neutral amino-

acids (Singh and Ecker, 2018). Slc7a5 silencing barely affected proliferation of B16F10 melanoma cells but promoted a strong and reproducible inhibition of melanogenesis.

To understand the key role of SLC7A5 in the transport of amino-acids, thyroid hormones and metabolites, as well as its involvement in cancer cell survival/proliferation, huge efforts have been made to identify SLC7A5 inhibitors (Wang and Holst, 2015). To date, dozens of such inhibitors have been validated.

Testing BCH, the first in class SLC7A5 inhibitor (Kim *et al.*, 2008) and JPH203, an inhibitor in clinical trial (Oda *et al.*, 2010), we have been able to demonstrate that both inhibitors efficiently inhibited pigmentation in B16F10 melanoma cells.

Concerning the mechanism by which the inhibition of Slc7a5 affected melanogenesis, we did not observe an inhibition of the expression of melanogenic enzymes, Tyr, Tyrp1 and Dct. On the contrary, we observed that both genetic and pharmacological inhibition of Slc7a5 induces an increase in Tyrp1 expression. As there no change in mRNA level was observed, we can suggest that Slc7a5 inhibition impaired the targeting of Tyrp1 to proteasome or lysosome degradation compartments, as reported for tyrosinase (Watabe *et al.*, 2004, Fujita *et al.*, 2009). Our data also ruled out the possibility that BCH inhibited directly the tyrosinase activity.

SLC7A5 transports tyrosine, the key substrate for melanin synthesis. Therefore, SLC7A5 inhibition might reduce cellular tyrosine level, even though tyrosine is not an essential amino acid, melanocytes cannot synthetize tyrosine from phenylalanine. Furthermore, as melanogenesis takes place in melanosomes, tyrosine must be transported into these organelles. Tyrosine transport activity has been identified, but the nature of the transporter remains elusive. Proteomic analysis of melanosomes (Basrur *et al.*, 2003) and immunoprecipitation of intact melanosomes (data not shown) both failed to validate the presence of SLC7A5 in the organelles. Additionally, SLC7A5 was reported to regulate the efflux of L-glutamine out of cells and the transport of L-leucine into the cell. Through this activity SLC7A5 plays a key role in the control

of mTOR and autophagy (Nicklin *et al.*, 2009). Interestingly, autophagy was described to regulate melanogenesis, as its activation leads to melanosome degradation and inhibition of melanin synthesis (Ho and Ganesan, 2011). Therefore, it can be proposed that SLC7A5 inhibition activates autophagy that is responsible for the inhibition of pigmentation. We assessed this hypothesis by combining autophagy inhibitors (3-MA or Chloroquine) with BCH, or SLC7A5 siRNA. However, autophagy inhibitors strongly potentiate the anti-proliferative effects of SLC7A5 inhibition (data not shown), preventing reliable interpretation of the results. Nevertheless, BCH at 5 and 10 mM induced a conversion of LC3-I to LC3-II demonstrating an activation of autophagy and validating the inhibition of Slc7a5 by BCH (Supplementary Figure 4d).

Finally, we have been able to show that BCH prevented pigmentation in two different human cell models. BCH also inhibited pigmentation in reconstructed human epidermis, without affecting epidermis structure or keratinisation, predicting no major adverse effects.

Taken together, these data indicate that SLC7A5 plays an important role in melanin production and is amenable to pharmacological targeting for treatment of hyperpigmentation conditions.

MATERIAL AND METHODS

Cell culture and chemicals

Mouse B16F10 and Human 501Mel melanoma cells were cultured in Dulbecco's modified Eagle's medium (DMEM) supplemented with 7% Fetal Bovine Serum and 1% Penicillin/Streptomycin. Human MNT1 melanoma cells were cultured as described (Yasumoto *et al.*, 2004). Normal Human Melanocytes were isolated from foreskin and cultured in MCDB medium as described (Bonet *et al.*, 2017). Cells were tested every 4 weeks for mycobacterial presence. BCH (Tocris, France) and Kojic acid (Sigma, France) were resuspended in water at

50mM, and JPH203 (Selleckchem, France) was resuspended in DMSO at a 50mM stock solution.

Cell viability

Cell viability was evaluated using CellTiter Aqueous One Solution Cell Proliferation Assay (Promega, France) as recommended by the supplier.

Gene silencing and induction of pigmentation

Cells were transfected with 50nM siRNAs to SLC7A5, MITF or control siRNAs (ON-TARGETplus, Dharmacon) using HiPerfect transfection reagent (Qiagen, France). When indicated, Forskolin (20µM) and IBMX (100µM) were added to induce pigmentation on B16F10 cells. 48 hours later, medium was removed, and cells were used for western blot, quantitative PCR, melanin content analyses, immunofluorescence or brightfield imaging.

Protein expression

Proteins were analyzed by SDS-PAGE and transferred on PVDF membranes (Sigma, France). The antibodies used were as follow: beta-actin (ab8226), MITF (ab12039) and Tyrosinase (ab738) from Abcam, Rab27a (#69295) and HSP90 (#4874) from Cell Signaling Technologies, SLC7A5 (sc-374232) and TYRP1 (sc-166857) from Santa Cruz. Signals were detected with horseradish peroxidase conjugated secondary antibodies using ECL detection kit and quantified by digital imaging (Fuji LAS4000).

Melanin content

Cells were detached with 0.05% Trypsin-EDTA solution (Thermo Scientific, France) and solubilized in NaOH 0.5N. Optical density was measured at 405nm using melanin standard as a reference. Melanin content was normalized to the protein content.

Immunofluorescence and confocal analysis

Cells were fixed with Paraformaldehyde 4%, permeabilized with Triton 0.1% and incubated with anti-TYRP1 antibody (Santa Cruz, sc-58438). Fluorescent signal was revealed using Alexa Fluor 594 labeled secondary antibody (Thermo Scientific, France). Images were obtained using confocal Nikon A1R microscope (40X oil immersion lens).

Real-time quantitative PCR

Real-time quantitative PCR was carried out with SYBR Green using a StepOne Real-Time PCR System (Thermo Scientific, France). Results were normalized using GAPDH. Primer sequences are available upon request.

L-DOPA activity

Proteins were resuspended in 0.1M Sodium Phosphate pH 6.8, supplemented with 5mM L-DOPA. After incubation for 1 hour at 37°C, optical density was read at 475nm.

Reconstructed Human Pigmented Epidermis

Phototype VI Reconstructed Human Pigmented Epidermis (Sterlab, France) were treated with BCH or vehicle for 7 days. 10µm cryosections were used to visualize melanin using Fontana-Masson stain kit (Interchim, France). Images were taken with a Nikon microscope and a 20X lens. Melanin content was quantified after solubilization of epidermis in Solvable® solution (PerkinElmer, France), and melanin content was quantified as described above.

Statistical analyses

All data are presented as mean ± SD. A one-way ANOVA test was used for all the experiments, followed by a Dunnett's multiple comparisons test.

Data Availability

Datasets related to this article can be found at [https://www.ncbi.nlm.nih.gov/geo/query/acc.cgi?acc=GSE61967], hosted at GEO Omnibus (Laurette *et al.*, 2015) and at [https://portals.broadinstitute.org/ccle/data], hosted by the BROAD institute.

CONFLICT OF INTEREST.

RB received honorarium from Nunii.

ACKNOWLEDGEMENT.

This work was supported by grants from INSERM, the University of Nice-Sophia-Antipolis and Nunni laboratoire. We thank Dr Kurzen for providing skin sample for melanocyte preparation, Marie Irondelle from the imaging facility of C3M, Jean-François Peyron and Marielle Nebout for providing JPH203.

AUTHOR CONTRIBUTIONS

Conceptualization: CB and RB**. Funding acquisition and project administration**: FM, CB, RB. **Investigation**: CG obtained the majority of data presented herein and was assisted by FS, JL, KB, CH. **Writing**: original draft, CB and RB. Review and editing, CG. All authors reviewed and approved the final version of the manuscript before its submission for publication.

REFERENCES

Basrur V, Yang F, Kushimoto T, Higashimoto Y, Yasumoto K, Valencia J*, et al.* (2003) Proteomic analysis of early melanosomes: identification of novel melanosomal proteins. *J Proteome Res* 2:69-79.

Baxter LL, Watkins-Chow DE, Pavan WJ, Loftus SK (2019) A curated gene list for expanding the horizons of pigmentation biology. *Pigment Cell Melanoma Res* 32:348-58.

Bonet C, Luciani F, Ottavi JF, Leclerc J, Jouenne FM, Boncompagni M*, et al.* (2017) Deciphering the Role of Oncogenic MITFE318K in Senescence Delay and Melanoma Progression. *J Natl Cancer Inst* 109.

Cheli Y, Ohanna M, Ballotti R, Bertolotto C (2010) Fifteen-year quest for microphthalmia-associated transcription factor target genes. *Pigment Cell Melanoma Res* 23:27-40.

Fujita H, Motokawa T, Katagiri T, Yokota S, Yamamoto A, Himeno M*, et al.* (2009) Inulavosin, a melanogenesis inhibitor, leads to mistargeting of tyrosinase to lysosomes and accelerates its degradation. *J Invest Dermatol* 129:1489-99.

Goding CR, Arnheiter H (2019) MITF-the first 25 years. *Genes Dev* 33:983-1007.

Ho H, Ganesan AK (2011) The pleiotropic roles of autophagy regulators in melanogenesis. *Pigment Cell Melanoma Res* 24:595-604.

Hume AN, Seabra MC (2011) Melanosomes on the move: a model to understand organelle dynamics. *Biochem Soc Trans* 39:1191-6.

Kim CS, Cho SH, Chun HS, Lee SY, Endou H, Kanai Y*, et al.* (2008) BCH, an inhibitor of system L amino acid transporters, induces apoptosis in cancer cells. *Biol Pharm Bull* 31:1096-100.

Kondo T, Hearing VJ (2011) Update on the regulation of mammalian melanocyte function and skin pigmentation. *Expert Rev Dermatol* 6:97-108.

Laurette P, Strub T, Koludrovic D, Keime C, Le Gras S, Seberg H*, et al.* (2015) Transcription factor MITF and remodeller BRG1 define chromatin organisation at regulatory elements in melanoma cells. *Elife* 4.

Miyamura Y, Coelho SG, Wolber R, Miller SA, Wakamatsu K, Zmudzka BZ*, et al.* (2007) Regulation of human skin pigmentation and responses to ultraviolet radiation. *Pigment Cell Res* 20:2-13.

Nicklin P, Bergman P, Zhang B, Triantafellow E, Wang H, Nyfeler B*, et al.* (2009) Bidirectional transport of amino acids regulates mTOR and autophagy. *Cell* 136:521-34.

Oda K, Hosoda N, Endo H, Saito K, Tsujihara K, Yamamura M*, et al.* (2010) L-type amino acid transporter 1 inhibitors inhibit tumor cell growth. *Cancer Sci* 101:173-9.

Ohanna M, Cerezo M, Nottet N, Bille K, Didier R, Beranger G*, et al.* (2018) Pivotal role of NAMPT in the switch of melanoma cells toward an invasive and drug-resistant phenotype. *Genes Dev* 32:448-61.

Singh N, Ecker GF (2018) Insights into the Structure, Function, and Ligand Discovery of the Large Neutral Amino Acid Transporter 1, LAT1. *Int J Mol Sci* 19.

Sitaram A, Marks MS (2012) Mechanisms of protein delivery to melanosomes in pigment cells. *Physiology (Bethesda)* 27:85-99.

Wang Q, Holst J (2015) L-type amino acid transport and cancer: targeting the mTORC1 pathway to inhibit neoplasia. *Am J Cancer Res* 5:1281-94.

Watabe H, Valencia JC, Yasumoto K, Kushimoto T, Ando H, Muller J*, et al.* (2004) Regulation of tyrosinase processing and trafficking by organellar pH and by proteasome activity. *J Biol Chem* 279:7971-81.

Yasumoto K, Watabe H, Valencia JC, Kushimoto T, Kobayashi T, Appella E*, et al.* (2004) Epitope mapping of the melanosomal matrix protein gp100 (PMEL17): rapid processing in the endoplasmic reticulum and glycosylation in the early Golgi compartment. *J Biol Chem* 279:28330-8.

Figure Legends.

Figure 1. SLC7A5 is a new MITF target gene.

a) UCSC browser image capture of the SLC7A5 promoter region from MITF (Black), H3K27ac and H3K4me3 (purple) ChIP-seq experiments. b to c. MITF and SLC7A5 expression in cells after transfection with control (siCt) or MITF (siMITF) siRNA. Messenger quantification in B16F10 cells (b) by real-time quantitative PCR. Values are mean ± SD from three different experiments performed in triplicate. Protein expression evaluation by western-blot in B16F10 cells (c).

Figure 2. SLC7A5 silencing affects melanogenesis.

a) Evaluation of SLC7A5 expression by western-blot of B16F10 cells after transfection with control (si Ct) or two different SLC7A5 (si1 and si2) si RNA. b) Bright field images taken from B16F10 cells after transfection with siCt or si2. Bar represents 100µm. c) Melanin content in B16F10 cells after SLC7A5 silencing. Values were normalized per amount of proteins and calculated as percentage of the control condition (siCt). Values are mean ± SD from three different experiments. ****p<0.0001. d) Immunofluorescence labelling of Tyrp1 in B16F10 cells after transfection with control or SLC7A5 siRNA. Images were taken with a confocal microscope. Bar represents 50µm.

Figure 3. The specific inhibitor BCH also decreases cell pigmentation.

a) Measurement of cell viability in B16F10 cells after treatment with BCH. b) Quantification of melanin content in B16F10 cells treated with various doses of BCH. Values were normalized per amount of proteins and calculated as percentage of the basal condition. Values are mean ± SD from three different experiments. ****p<0.0001. c) Bright field images of B16F10 cells treated with vehicle or BCH at 10mM. Bar represents 100µm. d) Immunofluorescence labelling of Tyrp1 in B16F10 cells after treatment with vehicle or BCH at 10mM. Images were taken with a confocal microscope. Bar represents 50µm.

Figure 4. Comparison between BCH and Kojic Acid effects.

a) Measurement of melanin content in B16F10 cells treated with various doses of Kojic Acid. Values were normalized per amount of proteins and calculated as percentage of the basal condition (0). Values are mean ± SD from three different experiments. ***p<0.001. b) In vivo measurement of L-DOPA activity after treatment of B16F10 cells with BCH at 10mM or Kojic Acid (KA) at 1mM for 72 hours. Values were normalized per amount of proteins and calculated as percentage of the basal condition. Values are mean ± SD from three different experiments. **p<0.01. c) In vitro measurement of L-DOPA activity after addition of BCH at 10mM or Kojic Acid (KA) at 1mM to cell lysates from B16F10 cells. Values were normalized per amount of proteins and calculated as percentage of the basal condition. Values are mean ± SD from three different experiments *p<0.05.

Figure 5. BCH reduces pigmentation in several models of highly pigmented cells.

Measurement of melanin content in MNT1 cells (a) or in normal human melanocytes (b) treated with BCH at 5 or 10mM for 7 days. Values were normalized per amount of proteins and calculated as percentage of the control condition (0). Values are mean ± SD from three different experiments. **p<0.005 and *p<0.05. c) Macroscopic images of phototype VI reconstructed human pigmented epidermis (RHPE) after treatment with BCH at 5 or 10mM for 7 days. d) Bright field images of RHPE treated with BCH at 10mM for 7 days. e) Fontana-Masson staining of 10µM cryosections of RHPE after treatment with BCH at 10mM for 7 days. Bar represents 50µm. F) Measurement of melanin content in reconstructed human pigmented epidermis treated with BCH for 7 days. Values were normalized per amount of proteins and calculated as percentage of the control condition (0). Values are mean ± SD from three different experiments. ****p<0.0001.

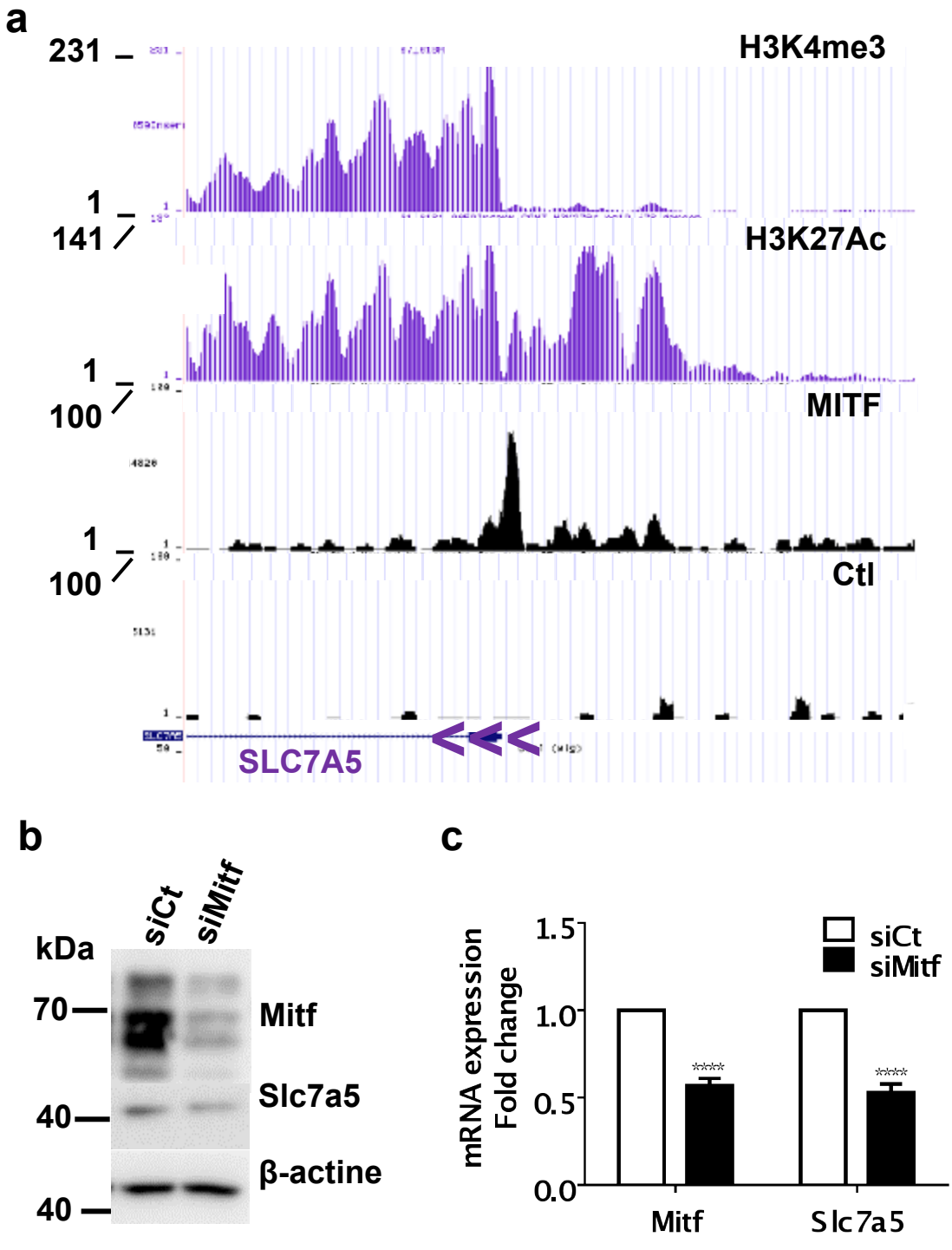
a
231
H3K4me3
1
141
H3K27Ac
1
100
MITF
1
100
Ctl
SLC7A5
b
siCt
siMitf
kDa
70
Mitf
Slc7a5
40
β-actine
40
c
mRNA expression
Fold change
1.5
1.0
0.5
0.0
siCt
siMitf
****
****
Mitf
Slc7a5

Figure 1

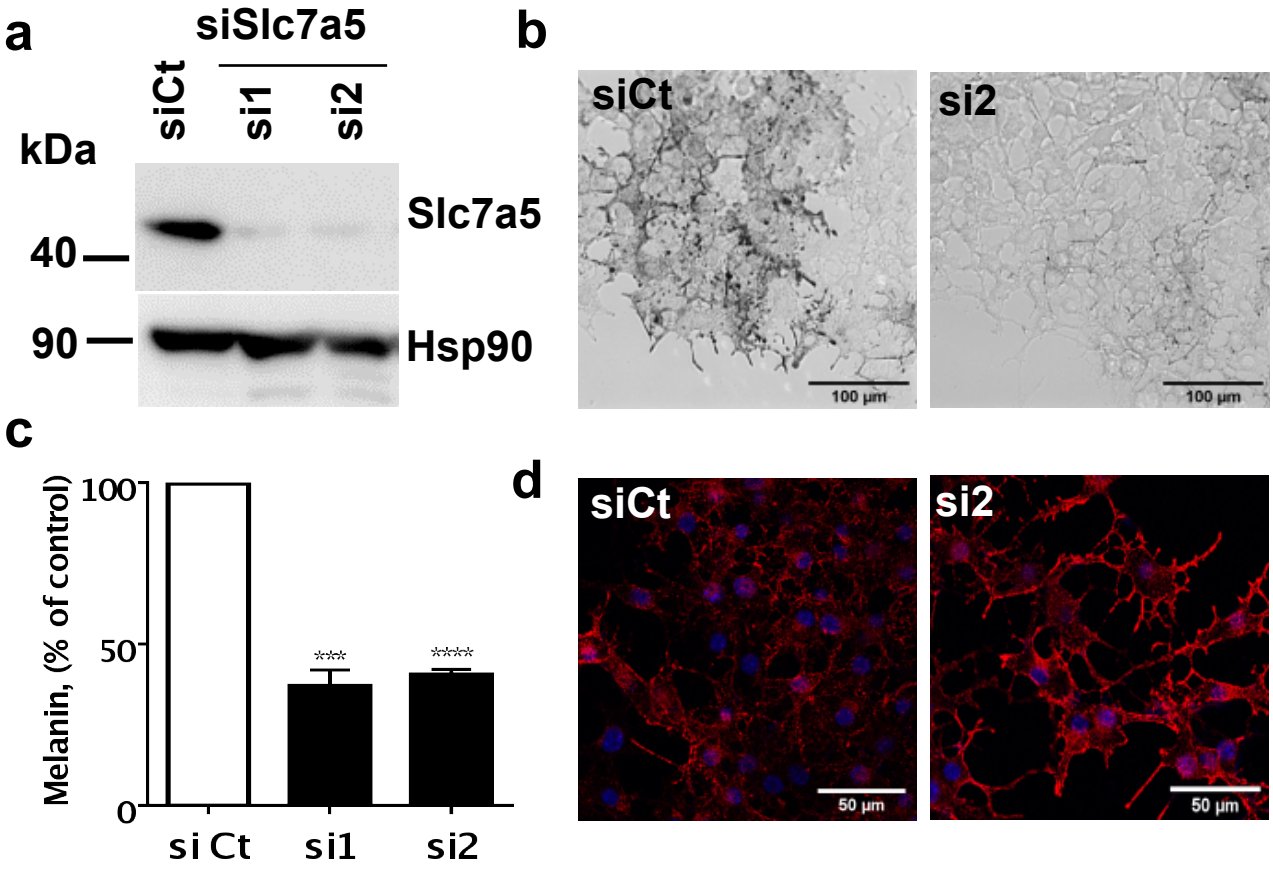
a
siSlc7a5
siCt
si1
si2
kDa
40
90
Slc7a5
Hsp90
b
siCt
si2
100 µm
100 µm
c
Melanin, (% of control)
100
50
0
****
****
si Ct
si1
si2
d
siCt
si2
50 µm
50 µm

Figure 2

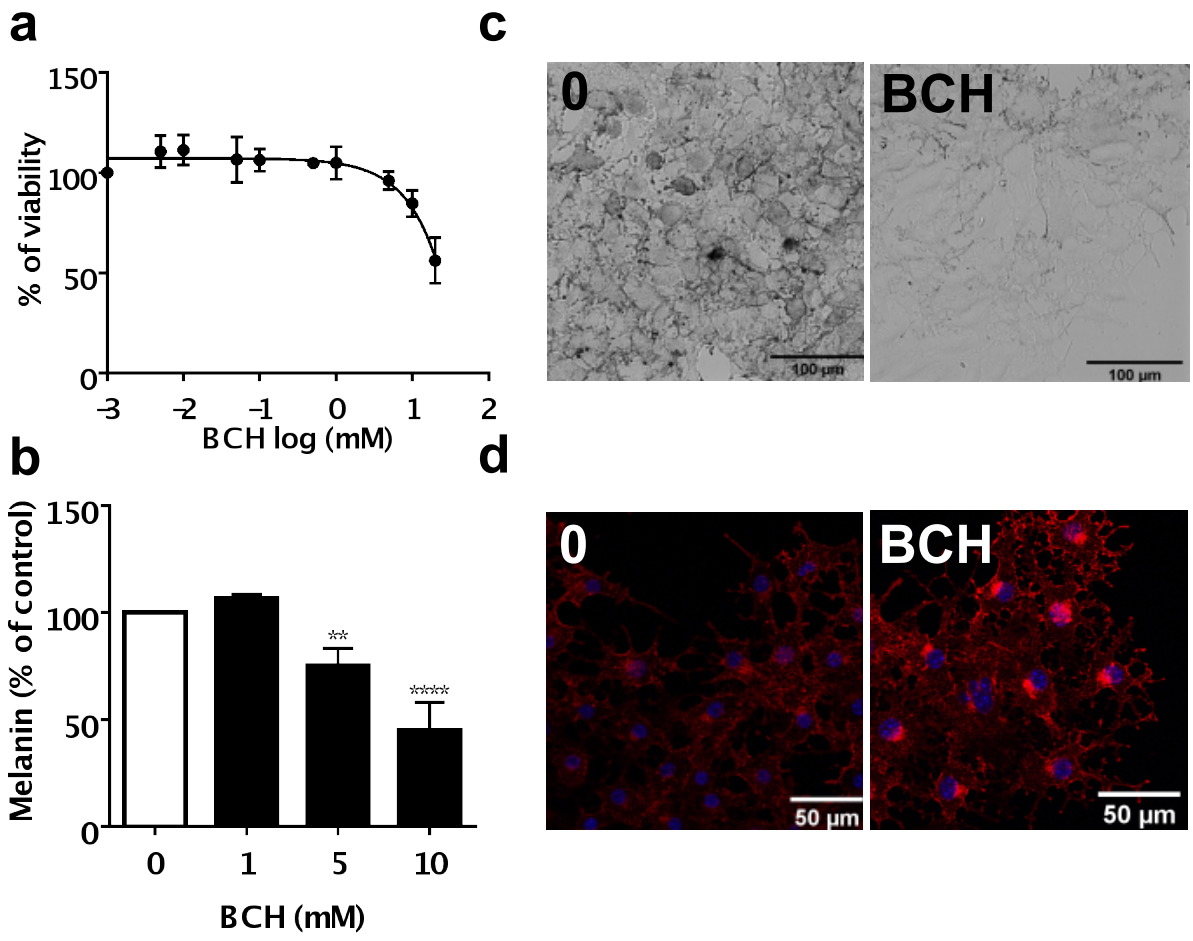
a
150
100
50
0
% of viability
-3
-2
-1
0
1
2
BCH log (mM)
b
Melanin (% of control)
150
100
50
0
**
****
0
1
5
10
BCH (mM)
c
0
BCH
100 µm
100 µm
d
0
BCH
50 µm
50 µm

Figure 3

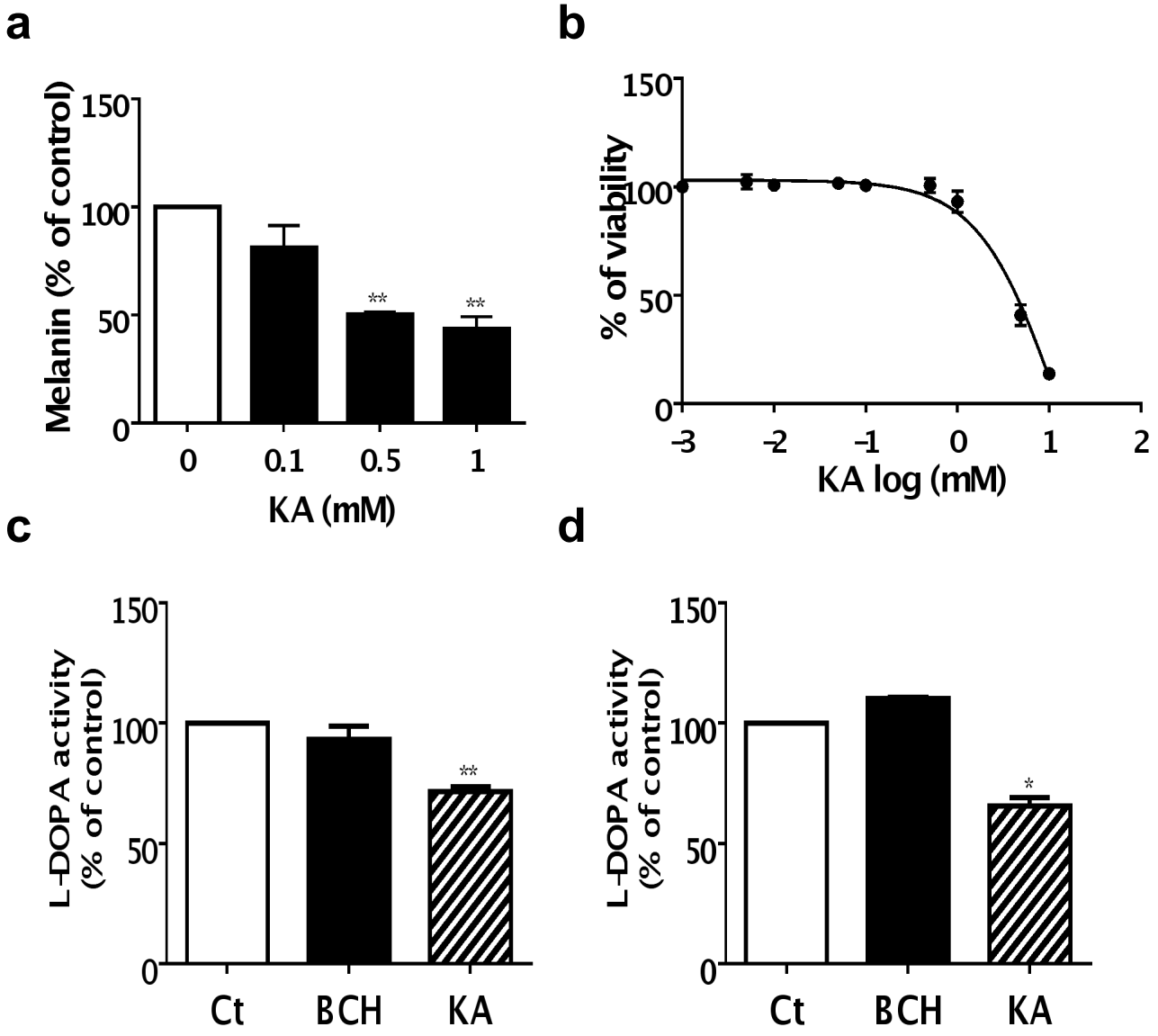
a
Melanin (% of control)
150
100
50
0
**
**
0
0.1
0.5
1
KA (mM)
b
% of viability
150
100
50
0
-3
-2
-1
0
1
2
KA log (mM)
c
L-DOPA activity (% of control)
150
100
50
0
**
Ct
BCH
KA
d
L-DOPA activity (% of control)
150
100
50
0
*
Ct
BCH
KA

Figure 4

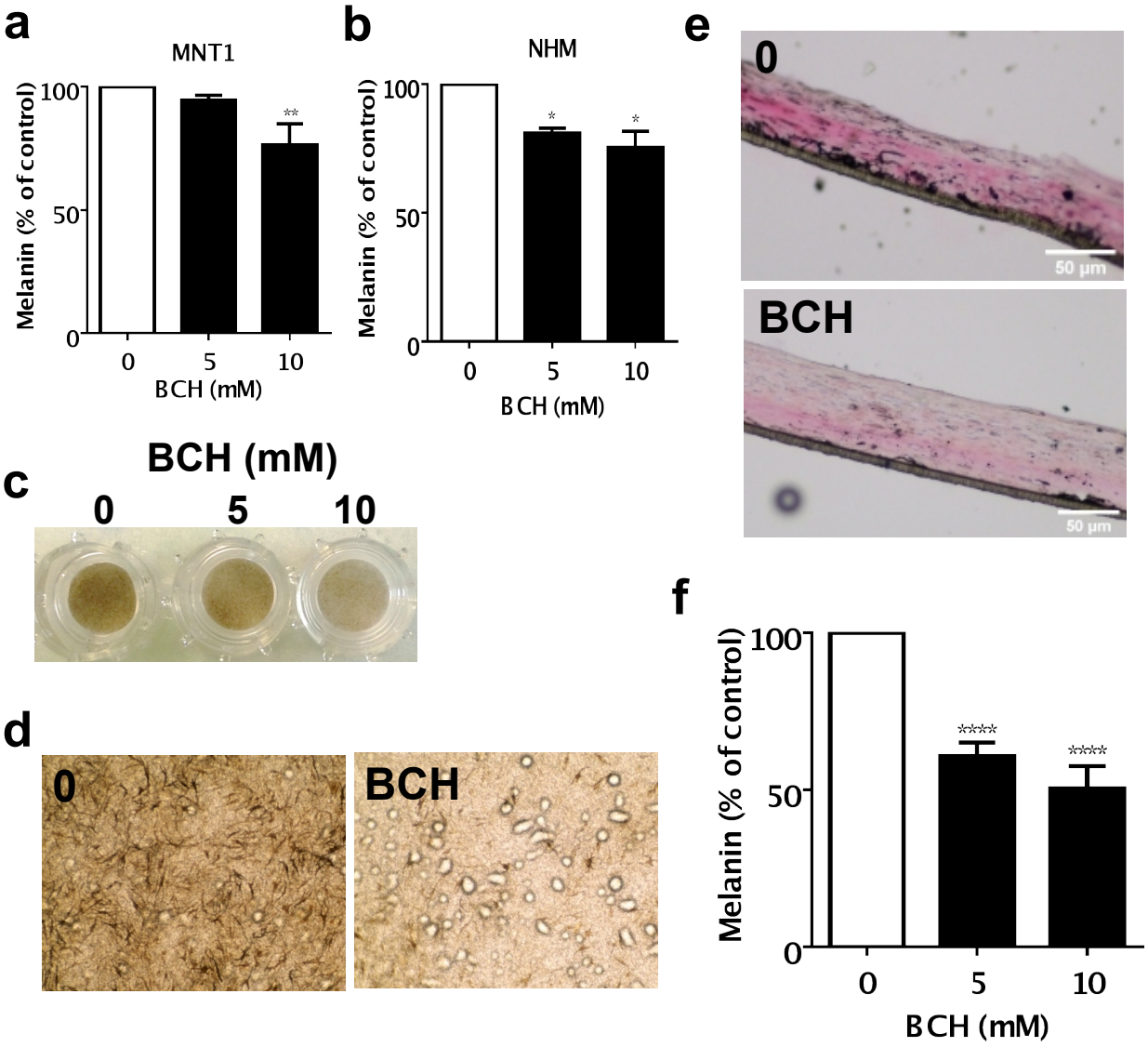
a
MNT1
Melanin (% of control)
100
50
0
**
0
5
10
BCH (mM)
b
NHM
Melanin (% of control)
100
50
0
*
*
0
5
10
BCH (mM)
e
0
50 µm
BCH
50 µm
c
BCH (mM)
0
5
10
d
0
BCH
f
Melanin (% of control)
100
50
0
****
****
0
5
10
BCH (mM)

Figure 5

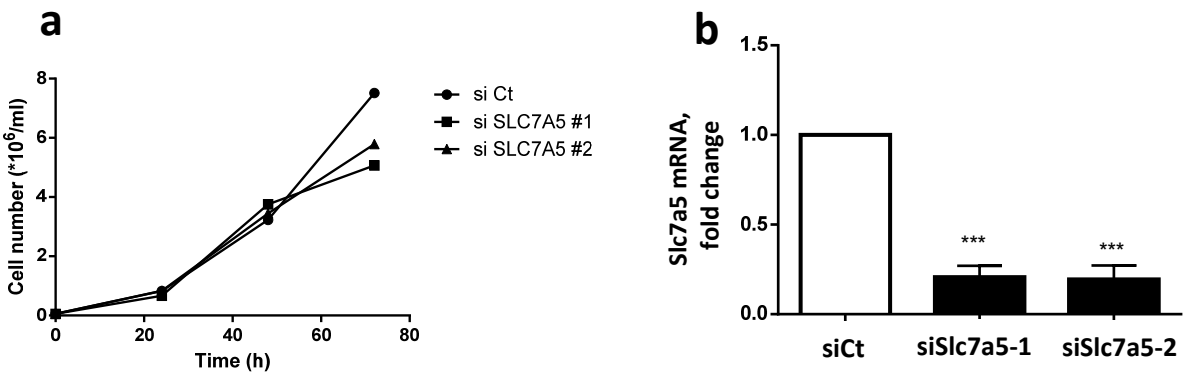

Supplemental Figure 1

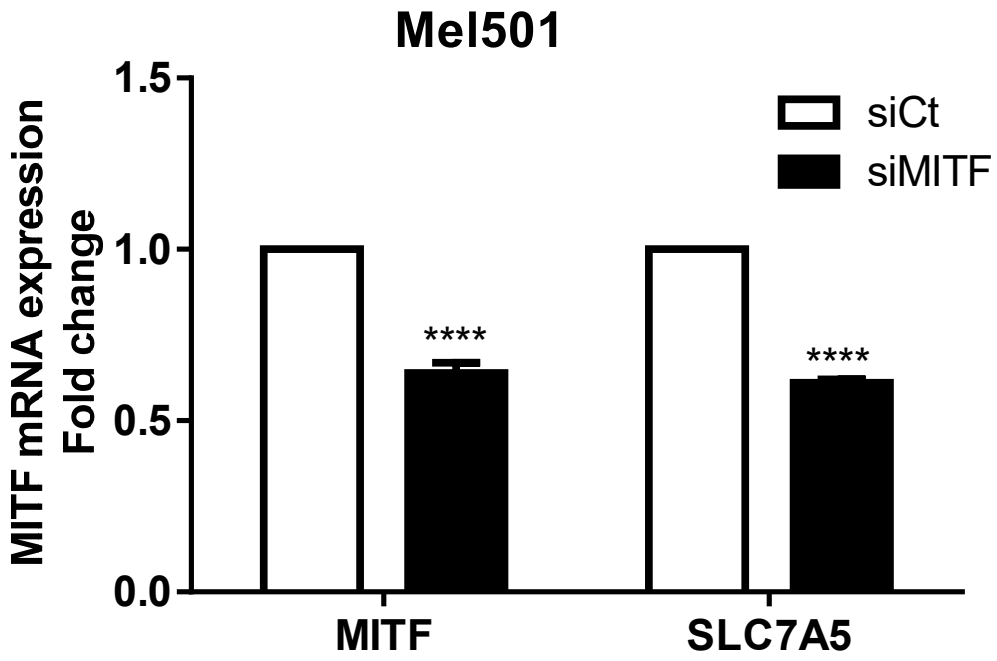

Supplemental Figure 2

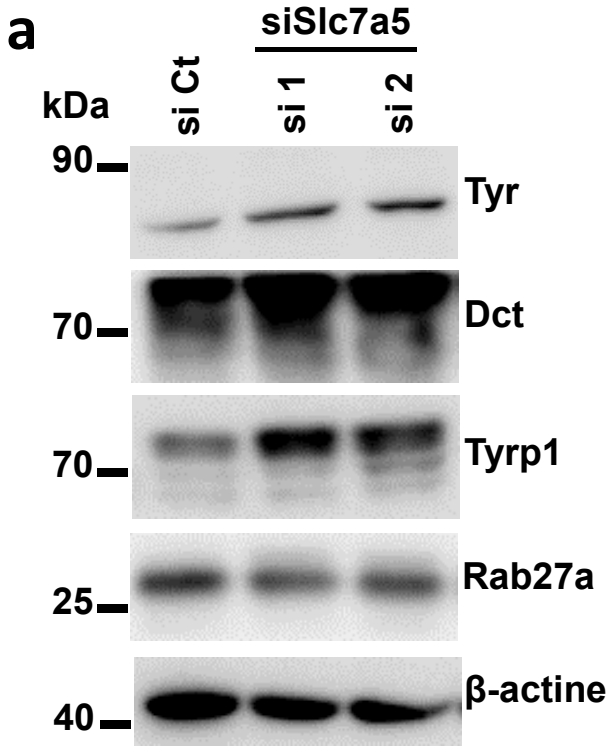

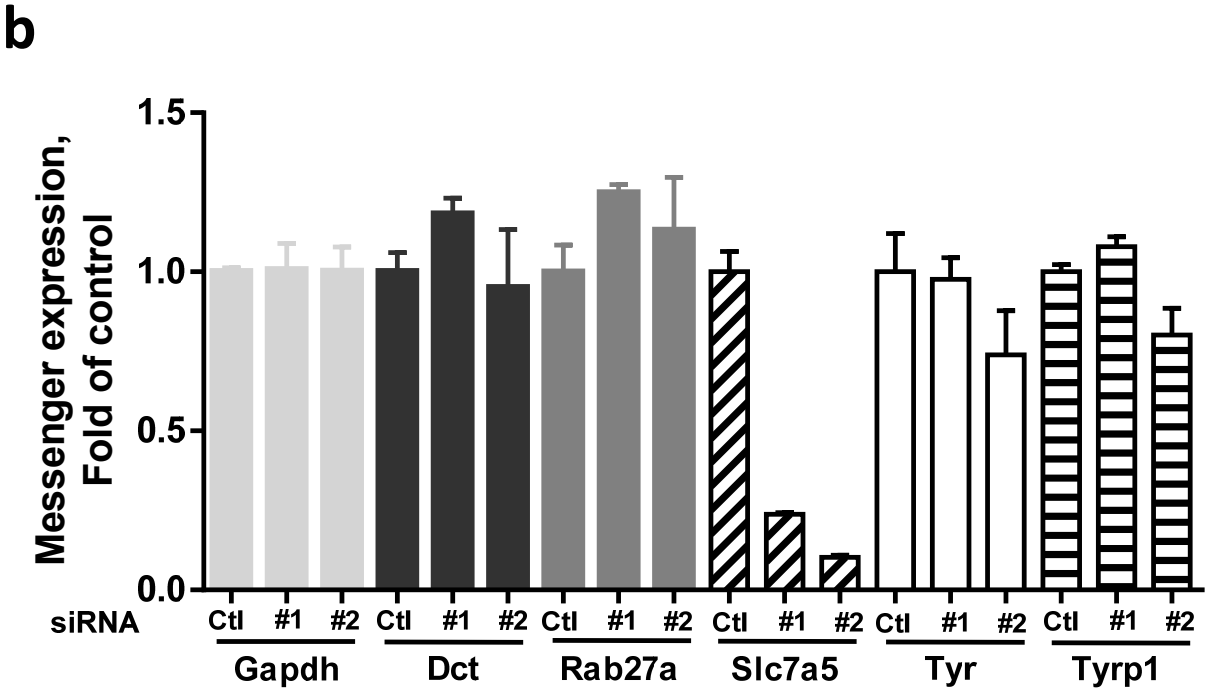

Supplemental Figure 3

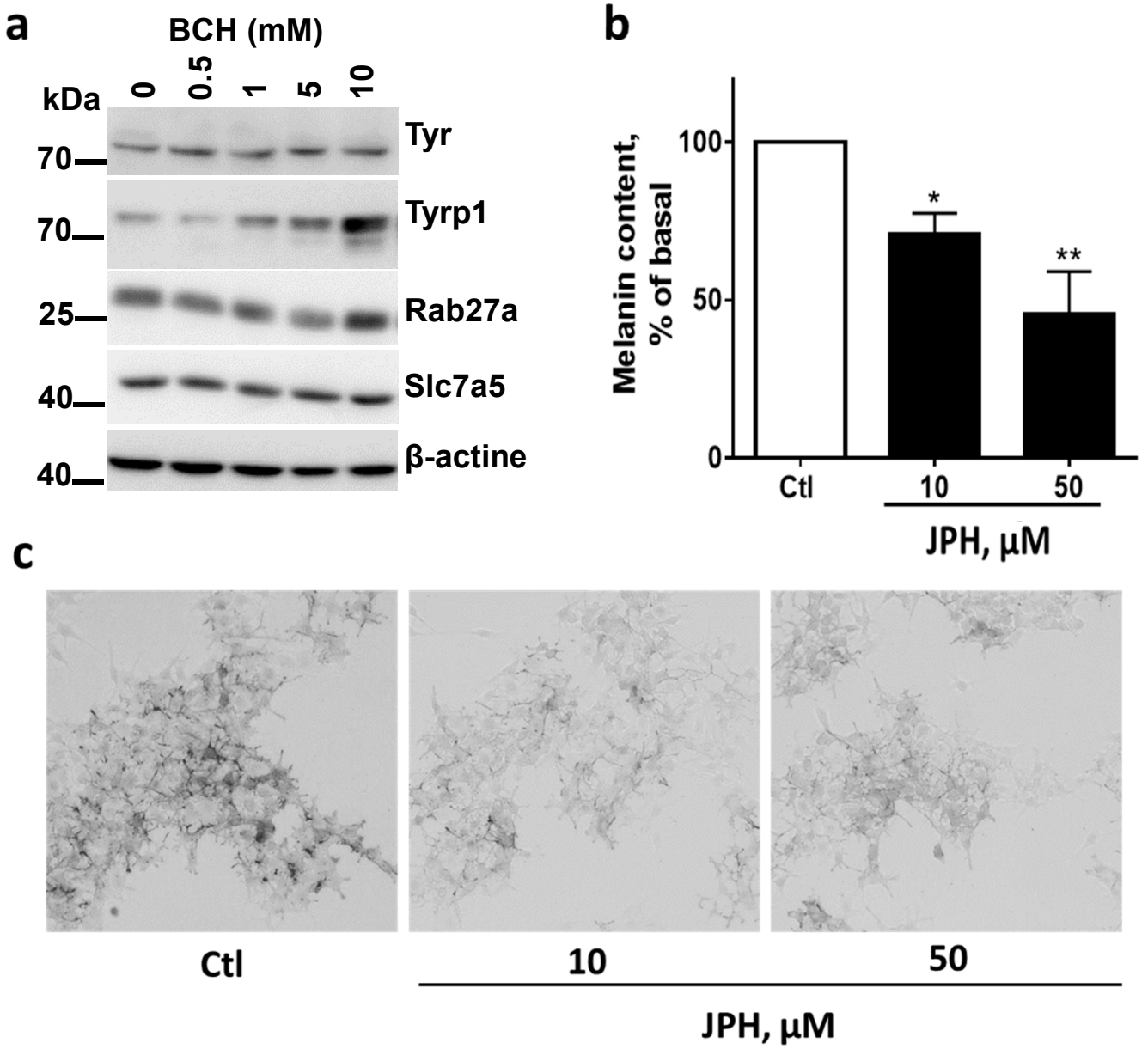

Supplemental Figure 4

GO biological process complete	Fold Enrichment	FDR
developmental pigmentation (GO:0048066)	7.51	7.36E-08
pigment accumulation (GO:0043476)	7.51	0.03
cellular pigment accumulation (GO:0043482)	7.51	0.03
coenzyme A metabolic process (GO:0015936)	7.01	0.02
phagosome acidification (GO:0090383)	6.98	9.55E-05
melanin biosynthetic process (GO:0042438)	6.94	0.04
pigment cell differentiation (GO:0050931)	6.79	4.99E-05
error-free translesion synthesis (GO:0070987)	6.76	3.64E-03
mitochondrial electron transport (GO:0006122)	6.44	0.05
melanin metabolic process (GO:0006582)	6.44	0.05
melanocyte differentiation (GO:0030318)	6.15	0.01
error-prone translesion synthesis (GO:0042276)	6.01	0.01
intracellular pH reduction (GO:0051452)	5.76	9.40E-06
melanosome localization (GO:0032400)	5.64	0.01

Sup table 1. Gene ontology enrichment analysis, using Panther classification system (http://pantherdb.org/) of the 946 genes that contain a MITF binding site (Min read 30) in their promoter (-2000/+150) and are positively correlated with MITF in the 61 melanoma cell panel of the CCLE, Broad institute.

#Chr	Annotation	Distance to TSS	max read	Gene Name	siMITF 501	simitf B16
chr3	promoter-TSS (NM_001271148)	-829	42	ST3GAL6	-1.146	-1.405
chr3	promoter-TSS (NM_006100)	-316	133	ST3GAL6	-1.146	-1.405
chr11	promoter-TSS (NM_000372)	-1	111	TYR	-1.723	-1.411
chr15	promoter-TSS (NM_183234)	-84	39	RAB27A	-1.860	-1.751
chr15	promoter-TSS (NM_183235)	-901	40	RAB27A	-1.860	-1.751
chr2	promoter-TSS (NM_001042467)	-23	70	MLPH	-2.309	-1.050
chr16	promoter-TSS (NM_003486)	-164	76	SLC7A5	-1.921	-1.024

Sup table 2. Final gene list was generated by applying additional filters (log Fold change after siMITF <-1, in both 501Mel and B16F10 cells). TSS is transcriptional start site.

Supplemental figure 1

a. Measurement of cell proliferation by flow cytometry in B16F10 cells transfected with control (siCt) or Slc7a5 (si1 and si2) for 24, 48 or 72 hours.

b. mRNA expression of Slc7a5 in B16F10 mouse melanoma cells after transfection with control (siCt) or Mitf (siMitf) siRNA for 72 hours by real-time quantitative PCR. Values are mean ± SD from three different experiments performed in triplicate. ***$p<0.001$.

Supplemental figure 2

Quantification of Mitf and Slc7a5 mRNA in B16F10 cells after Mitf silencing.

Supplemental figure 3

Analysis of melanogenic protein expression in B16F10 cells after transfection with control or Slc7a5 siRNA, by western-blot (a) or by qPCR (b)

Supplemental figure 4

a) Analysis of melanogenic protein and Slc7a5 expression by western blot in B16F10 cells after treatment with various doses of BCH. b) Quantification of melanin content in B16F10 cells treated with various doses of JPH203. Values were normalized per amount of proteins and calculated as percentage of the basal condition. Values are mean ± SD from three different experiments. *$p<0.05$, **$p<0.01$. c) Bright field images of B16F10 cells treated with vehicle or JPH203 at 50µM. Bar represents 10µM. d) Analysis of LC3-I to LC3-II conversion in B16F10 cells exposed to the indicated concentrations of BCH. Gapdh was used as loading control.